Malaysian Journal of Mathematical Sciences 10(S) February: 443–458 (2016)
Special Issue: The 3^{rd} International Conference on Mathematical Applications in Engineering 2014 (ICMAE'14)

MALAYSIAN JOURNAL OF MATHEMATICAL SCIENCES
Journal homepage: http://einspem.upm.edu.my/journal

Buckling Analysis of Isotropic Circular Plate with Attached Annular Piezoceramic Plate

Noh, S.*[1], Abdalla, M. M.[1,2], and Waleed, W. F.[2]

[1]*Department of Mechanical Engineering, International Islamic University, Malaysia*
[2]*Department of Aerospace Structures and Materials, Delft University of Technology, The Netherlands*

E-mail: syednoh@iium.edu.my
**Corresponding author*

ABSTRACT

A buckling analysis of an isotropic circular plate with piezoceramic annular plate attached to it is presented. The annular plate is attached at the circular plate edge so that the radius of the circular plate is the inner radius of the annular plate. The piezoceramic annular plate is used as the radial in-plane load source. The radial and hoop stresses are found to be depends on the radial throughout the annular region while constants throughout the circular regions. The governing equations is solved approximately using finite difference method. The solutions to be found to be in good agreement with results from FEM analysis. A parametric study also presented.

Keywords: Circular, Annular, Piezoelectric, Intermediate Buckling, Finite Difference Method.

1. Introduction

Plate buckling problem has been a classical problem in solid mechanics. There are great many literature and books (Wang et al., 2005) that deals with

plate buckling problem. Many of the reported annular plate buckling are formulated with the in-plane condition of both inner edge and outer edge are the similar, i.e. at both edge the plate is allowed to move in-plane and loaded with the same magnitude of load. This case will lead to a uniform stress distribution throughout the plate. This will lead to governing equation which the differential equation that could be solved analytically. However, for an annular plate with different in-plane condition, the stresses are varied with the radius which complicate the governing equation and the solution is not analytically available. Mansfield (Mansfield, 1960) reported on the plate buckling analysis with considering such stresses distribution throughout the plate. However, he did the buckling analysis for infinite annular plate which simplified the governing buckling equation and the analytical solution for such problem is available. He also claimed that the solution is also applicable to a similarly loaded finite annular plate if there is a member of the requisite tensile stiffness supporting the outer circle. In other reports, Ramaiah and Vijayakumar (Ramaiah and Vijayakumar, 1974) have investigated the elastic stability of annular plates under uniform compressive forces along the outer edge for all nine combinations of clamped, simply supported and free edges conditions. They employed the Rayleigh-Ritz method with simple polynomials as admissible function. Later, there are researchers did analytical approach in solving buckling problems where the in-plane loads are not uniformly distributed across the plate (Sheng-li and Ai-shu, 1984, Shi-rong, 1992). Qin Sheng-li and Zhang Ai-shu (Sheng-li and Ai-shu, 1984) have reported on the problem of unsymmetrical buckling of an annular thin plate under the action of in-plane pressure and transverse load. They used the method of multiple scales that is similar to what Kiang Fu-ru (Kiang, 1980) used in his analysis. Although they only showed the application of their analysis for circular plate subjected to the in-plane radial pressures that uniformly distributed over the plate boundaries ($N_{11} = N_{22} = -\mathrm{N} =$ constant, and $N_{12} = 0$) and also subjected to uniform pressure that acts on the plate surface, it may be etxended to a radius dependent in-plane load. Li Shi-rong (Shi-rong, 1992) has reported on study of the axisymmetric nonlinear vibration and thermal buckling of a uniformly heated isotropic plate with a completely clamped outer edge and a fixed rigid mass along the inner edge. He used both parametric perturbation technique and finite different method to obtain the nonlinear response of the plate-mass system and the critical temperature in the mid plane at which the plate is in buckled state. Recently, Coman and Haughton (Coman and Haughton, 2006a,b) have presented a reports on annular plate with simply supported inner edge and free outer edge and the tensile load is applied at the inner edge. They used compound matrix methods to solve the buckling governing equation. Although, there are efforts in solving buckling problems of annular plate that consider the stresses distribution which is not uniform but to the authors knowledge

it is confined to the annular plate problems. There are also condition where the stresses for curcular plate behave similarly which is dependent on radial direction such as circular plate buckling under intermediate radial load. Such conditions may be realized if the annular regions is heated or through application of annular piezoceramic materials. Aung and Wang (Aung and Wang, 2005) have reported on the buckling of circular plate under intermediate and radial edge loads for various boundary conditions. However, they restricted their problems either the stresses at annular region is uniform or zero. An annular plate with two different edge load will always give variations throughout the plates. To the authors knowledge, the analysis of intermediate radial loads that consider the variation of the stresses at the annular region is yet to be done. Therefore, it is of interest of this paper to address the buckling of circular plate under intermediate radial loads. The intermediate radial loads is realized through application of piezoceramic materials as its annular region. The outer edge is clamped. A parametric study also been done to show the effects of some geometric parameters on the buckling loads.

2. Formulations

2.1 Basic Relations

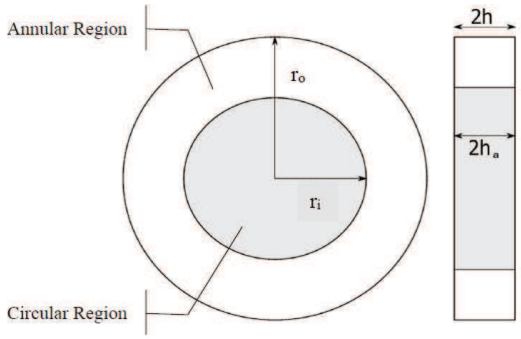

Figure 1: Circular plate with annular plate attached at its edge

Fig. 1 shows the circular solid plate (grey region) with an annular plate (white region) attached at its edge. In the present analysis the cylindrical polar coordinate is adopted. The origin of the coordinate is located at the centre of the circular. The radius and the thickness of the solid circular plate are denoted by r_i and $2h$, respectively. While the outer radius and thickness of the ring are denoted by r_o and $2h_a$, respectively. The inner radius of the

annular plate is equal to the circular plate's radius, r_i. In the present analysis, the material used for the annular plate is a piezoceramic while for the circular plate is an isotropic alloy. The annular piezoceramic's two surfaces are coated with complete electrodes.

In most practical applications, the ratio of a circular plate radius to the thickness is more than ten where the plate is considered to be a thin plate. For a thin plate, Kirchhoff's hypotheses may be applied and the shear deformation and rotatory inertia can be omitted. Under these assumptions, the strain-mechanical displacement relations can be expressed as:

$$e_{11} = \frac{\partial u_0}{\partial r} - z\frac{\partial^2 w_0}{\partial r^2} = e_{11}^0 + z\kappa_{11} \tag{1}$$

$$e_{22} = \frac{u_0}{r} + \frac{1}{r}\frac{\partial v_0}{\partial \theta} - \frac{z}{r}\left(\frac{\partial w_0}{\partial r} - \frac{1}{r}\frac{\partial^2 w_0}{\partial \theta^2}\right) = e_{22}^0 + z\kappa_{22} \tag{2}$$

$$e_{12} = \frac{1}{2}\left(\frac{1}{r}\frac{\partial u_0}{\partial \theta} + \frac{\partial v_0}{\partial r} - \frac{v_0}{\theta}\right) = e_{12}^0 + \frac{z}{2}\kappa_{12} \tag{3}$$

where u_0, v_0 and w_0 are the mid-plane radial displacement, circumferential displacement and deflection, while e_{ij}^0 and κ_{ij} are the in-plane strain and curvature, respectively. The variation of stress throughout the thickness for isotropic thin plate are,

$$\sigma_{11}^{(s)} = \frac{E}{(1-\mu^2)}\left(e_{11}^{0(s)} + z\kappa_{11}^{(s)} + \mu\left(e_{22}^{0(s)} + z\kappa_{22}^{(s)}\right)\right) \tag{4}$$

$$\sigma_{22}^{(s)} = \frac{E}{(1-\mu^2)}\left(e_{22}^{0(s)} + z\kappa_{22}^{(s)} + \mu\left(e_{11}^{0(s)} + z\kappa_{11}^{(s)}\right)\right) \tag{5}$$

$$\sigma_{12}^{(s)} = \frac{E}{2\,(1-\mu)}\left(e_{12}^{0(s)} + z\kappa_{12}^{(s)}\right) \tag{6}$$

where E and μ the Young coefficient and Poisson ratio for the isotropic shim, respectively and subscript (s) denotes the solid circular region. The linear piezoceramic constitutive equations for a piezoceramic material with crystal symmetry class C_{6mm} (Tiersten, 1969) under the assumptions made above can be written as

$$\sigma_{11}^{(a)} = \frac{1}{s_{11}^E\left(1-\nu_p^2\right)}\left(e_{11}^{0(a)} + z\kappa_{11}^{(a)} + \nu_p\left(e_{22}^{0(a)} + z\kappa_{22}^{(a)}\right)\right) - \frac{d_{31}E_3^{(a)}}{s_{11}^E\left(1-\nu_p\right)} \tag{7}$$

$$\sigma_{22}^{(a)} = \frac{1}{s_{11}^E\left(1-\nu_p^2\right)}\left(e_{22}^{0(a)} + z\kappa_{22}^{(a)} + \nu_p\left(e_{11}^{0(a)} + z\kappa_{11}^{(a)}\right)\right) - \frac{d_{31}E_3^{(a)}}{s_{11}^E\left(1-\nu_p\right)} \tag{8}$$

$$\sigma_{12}^{(a)} = \frac{1}{2s_{11}^{E}\left(1+\nu_p\right)}\left(e_{12}^{0(a)} + z\kappa_{12}^{(a)}\right) \tag{9}$$

$$D_3 = d_{31}\left(e_{11}^{0(a)} + z\kappa_{11}^{(a)} + e_{22}^{0(a)} + z\kappa_{22}^{(a)}\right) + \epsilon_{33}^{T}E_3^{(a)} \tag{10}$$

where s_{ij}^{E} are the compliance constants, d_{ij} are the piezoelectric constants, ϵ_{ij}^{T} are the dielectric constants, e_{ij} are the strains components, σ_{ij} are the stresses components, D_i are the electric displacement components, E_i are the electric field components, $\nu_p = -\mathrm{s}_{12}^{E}/s_{11}^{E}$, and subscript (a) denotes the annular piezoceramic region.

Apart of the Kirchhoff's assumptions, a piezoceramic plate needs an extra assumptions. The assumption of electric field is constant across the thickness of piezoelectric layer violates the Maxwell static electricity equation. Wang et. al. (Wang et al., 2001) proposed that the electric potential varies in thickness of piezoelectric layer by a quadratic law, which satisfies the Maxwell static electricity equation. Therefore in the present analysis in addition to the Kirchhoff's assumptions for thin plate, for piezoceramic annular plate, the electric potential is assumed to varies with the thickness by the square law, i.e. $\phi = \phi_0 + \phi_1 z + \phi_2 z^2$ where ϕ_0, ϕ_1 and ϕ_2 are constants and the electric displacement is assumed to be constant with respect to the plate thickness, i.e. $\partial D_3/\partial z = 0$ (Huang et al., 2004, Huang, 2005). The constant in the equation of the electric potential can be determined from the electric potential boundary conditions on the piezoceramic layer surfaces, relations of electric displacement to electric potential from linear piezoelectric constitutive equations, Eq. (10) and the assumption of constant electric displacement in thickness. This follows the work of Huang (Huang et al., 2004, Huang, 2005). Therefore by using the piezoceramic constituve equation, the electric potential boundary conditions and the assumption on electric potential, the distribution of electric field for the piezoceramic ring can be determined. The electric potential boundary condition for the present piezoceramic ring are $\phi|_{z=h_a} = V$ and $\phi|_{z=-h_a} = 0$, where the surfaces of the plate are assumed to be fully coated with electrode. Thus, the distribution of electric field is

$$E_3^{(a)} = -\frac{V}{2h_a} - \frac{zd_{31}}{\epsilon_{33}^{T}s_{11}^{E}\left(1-\nu_p\right)\left(1-k_p^2\right)}\left(\kappa_{11}^{(a)} + \kappa_{22}^{(a)}\right) \tag{11}$$

where $k_p^2 = 2d_{31}^2\left(\epsilon_{33}^{T}s_{11}^{E}\left(1-\nu_p\right)\right)$ is the planar electromechanical coupling coefficient, and subscript (a) denotes the annular region.

The in-plane loads, N_{11}, N_{22} and N_{12} are defined as the integration of the stresses over thickness which results

$$N_{11}^{(s)} = A\left(e_{11}^{0(s)} + \mu e_{22}^{0(s)}\right) \tag{12}$$

$$N_{22}^{(s)} = A\left(e_{22}^{0(s)} + \mu e_{11}^{0(s)}\right) \tag{13}$$

$$N_{12}^{(s)} = Ge_{12}^{0(s)} \tag{14}$$

for isotropic plate, and

$$N_{11}^{(a)} = A_p\left(e_{11}^{0(a)} + \nu_p e_{22}^{0(a)}\right) + N_p \tag{15}$$

$$N_{22}^{(a)} = A_p\left(e_{22}^{0(a)} + \nu_p e_{11}^{0(a)}\right) + N_p \tag{16}$$

$$N_{12}^{(a)} = G_p e_{12}^{0(a)} \tag{17}$$

for piezoceramic plate. A, G are the strectching stiffness and shear modulus for isotropic plate, A_p and G_p are the stretching stiffness and shear modulus for piezoceramic plate and Np is the in-plane load due to the applied voltage which are defined as

$$A = \frac{2Eh}{(1-\mu)}; \frac{Eh}{(1+\mu)}; A_p = \frac{2h}{s_{11}^E\left(1-\nu_p^2\right)}; G_p = \frac{h}{s_{11}^E\left(1+\nu_p\right)} \text{and} N_p = \frac{Vd_{31}}{s_{11}^E\left(1-\nu_p\right)} \tag{18}$$

2.2 In-plane Load Distribution for Circular and Annular Plate

In the present analysis, the pre-buckling state of stress and strain is assumed to be axisymmetric such that $u = u(r)$ and $v = 0$. For such case, the Eq. (1)-Eq. (3) for strains becomes

$$e_{11}^0 = \frac{\partial u_0}{\partial r}; e_{22}^0 = \frac{u_0}{r} \text{and} e_{12}^0 = 0 \tag{19}$$

From radial component of the plate equlibrium equations along with Eq. (15)-Eq. (17) (or Eq. (12)-Eq. (14) for isotropic plate) and Eq. (19)

$$-\frac{1}{r}\left[\frac{\partial}{\partial r}\left(rN_{11}\right) + \frac{\partial N_{12}}{\partial \theta} - N_{22}\right] = 0 \frac{du^2}{dr^2} + \frac{1}{r}\frac{du}{dr} - \frac{u}{r^2} = 0 \tag{20}$$

which is a Cauchy-Euler equation. The general solution of the Eq. (20) is

$$u^{(a)} = \frac{C_1}{r} + C_2 r \tag{21}$$

where the coefficients C_1 and C_2 are determined from boundary conditions. Since the in-plane load is depends on the strain which in turn depends on

the mechanical displacement, therefore if the displacement is known then the in-plane load is also known.

For a solid circular plate, the first terms of Eq. (21) may produce singularity at the center of the plate. To avoid the singularity problem, the first term should be omitted thus the solution of Cauchy-Euler equation for a solid circular plate may be written as

$$u^{(a)} = C_4 r \tag{22}$$

If one substitute Eq. (22) into the in-plane load expression (Eq. (12)-Eq. (14)) as,

$$N_{11}^{(s)} = C_4 A\,(1+\mu) = N_{22}^{(s)} = N_s \tag{23}$$

which gave the in-plane load distributions for solid circular region. It reveals that the in-plane loads are independent of radius and uniformly distributed across the plate. In addition, the radial in-plane load is equal to circumferential in-plane load.

The constants C_1, C_2, and C_4 are determined by the boundary conditions of the plates. Here, the determination of the constants for a circular plate with applied intermediate radial load and clamped at outer edge is shown. The intermediate radial load may be realized by heating some annular portion of the plate or attaching with piezoelectric part. For present analysis, a circular plate is attached with an annular plate which surrounds it therefore by applying voltage on the annular plate may results tensional or compressed force to the circular plate. The boundary condition that being considered here is clamped outer plate while at interface between circular and annular plate, a matching condition is imposed. From clamped outer edge condition,

$$u^{(a)}\Big|_{r=r_o} = 0 \tag{24}$$

At interface circular - annular, the matching condition requires the radial in-plane load and radial displacement for both plate to be equal,

$$u^{(s)}\Big|_{r=r_i} = u^{(a)}\Big|_{r=r_i} \text{ and } N_{11}^{(s)}\Big|_{r=r_i} = N_{11}^{(a)}\Big|_{r=r_i} \tag{25}$$

Mathemathically manipulate these three equations (Eq. (24)-Eq. (25)) will give the constants C_1, C_2 and C_4 as

$$C_1 = -\frac{N_p r_i^2 r_o^2}{\left(\left(r_o^2 - r_i^2\right)\left(A_{11}^{(s)} + A_{12}^{(s)}\right) + r_o^2\left(A_{11}^{(a)} - A_{12}^{(a)}\right) + r_i^2\left(A_{11}^{(a)} + A_{11}^{(a)}\right)\right)} \tag{26}$$

$$C_2 = -\frac{C_1}{r_o^2} \tag{27}$$

$$C_4 = -\frac{C_1\left(r_o^2 - r_i^2\right)}{r_i^2 r_o^2} \tag{28}$$

Therefore the in-plane load distribution are,

$$N_{11}^{(a)} = \frac{N_p r_i^2 r_o^2}{\left(A\left(r_o^2 - r_i^2\right)(1+\mu) + A_p r_o^2\left(1-\nu_p\right) + A_p r_i^2\left(1+\nu_p\right)\right)} \times \left[\frac{A_p\left(1-\nu_p\right)}{r^2} + \frac{A_p\left(1+\nu_p\right)}{r_o^2}\right] - N_p \tag{29}$$

$$N_{22}^{(a)} = -\frac{N_p r_i^2 r_o^2}{\left(A\left(r_o^2 - r_i^2\right)(1+\mu) + A_p r_o^2\left(1-\nu_p\right) + A_p r_i^2\left(1+\nu_p\right)\right)} \times \left[\frac{A_p\left(1-\nu_p\right)}{r^2} + \frac{A_p\left(1+\nu_p\right)}{r_o^2}\right] - N_p \tag{30}$$

$$N_s = -\frac{N_p A(1+\mu)\left(r_o^2 - r_i^2\right)}{\left(A\left(r_o^2 - r_i^2\right)(1+\mu) + A_p r_o^2\left(1-\nu_p\right) + A_p r_i^2\left(1+\nu_p\right)\right)} \tag{31}$$

2.3 Governing Equation

In the present analysis, the shear in-plane load N_{12} is zero while the radial and circumferential in-plane load may be varied with radial direction. Under this condition, the thickness direction equilibrium equation for axisymmteric problem may be written as

$$D\nabla_r^4 w - N_{11}\frac{d^2w}{dr^2} - \frac{N_{22}}{r}\frac{dw}{dr} = 0 \tag{32}$$

where ∇_r^4 is the polar biharmonic operator which defined as

$$\nabla_r^4 \equiv \frac{d^4w}{dr^4} + \frac{2}{r}\frac{d^3w}{dr^3} - \frac{1}{r^2}\frac{d^2w}{dr^2} + \frac{1}{r^3}\frac{dw}{dr} \tag{33}$$

Eq. (32) is the general governing equations that govern a circular plate, thus either solid circular or annular plate is govern by Eq. (32). However, in the present analysis, the different appear in the definition of the in-plane load. For the annular region, the in-plane load is varied in radial direction (Eq. (29) and Eq. (30))but for solid circular region they are constant throughout the region (Eq. (31)).

2.4 Boundary Conditions

For the problem that is considered here the outer edge is clamped. At the interface between annular plate and circular plate a matching condition is imposed. The mathematical expressions for this condition are

1. at $r = r_o$, clamped outer edge

$$w^{(a)}\Big|_{r=r_o} = 0 \text{and } \frac{dw^{(a)}}{dr}\Big|_{r=r_o} = 0 \tag{34}$$

2. at $r = r_i$, matching condition

$$\begin{aligned} &w^{(a)}\Big|_{r=r_i} = w^{(s)}\Big|_{r=r_i}\ ;\ \frac{dw^{(a)}}{dr}\Big|_{r=r_i} = \frac{dw^{(s)}}{dr}\Big|_{r=r_i}\ ; \\ &M_{11}^{(a)}\Big|_{r=r_i} = M_{11}^{(s)}\Big|_{r=r_i} \text{ and } V_1^{(a)}\Big|_{r=r_i} = V_1^{(s)}\Big|_{r=r_i} \end{aligned} \tag{35}$$

where M_{11} and V_1 is radial bending moment and radial effective shear force which respectively given by

$$M_{11} = -D\left(\frac{d^2w}{dr^2} + \frac{\mu}{r}\frac{dw}{dr}\right) \tag{36}$$

and

$$V_1 = -D\left(\frac{d^3w}{dr^3} + \frac{1}{r}\frac{d^2w}{dr^2} - \frac{1}{r^2}\frac{dw}{dr}\right) + N_{11}\frac{dw}{dr} \tag{37}$$

3. Finite Difference Method

The problem of annular thin plate is actually a 2-D problems involving two independent variables namely radius, r and circumferential, θ. However, in the present analysis the dependent variable (the deflection w) is expand using the harmonic function. This reduce the problem into a 1-D problem involving one independent variables, the radius r. In the problem of 1-D circular plate, one may model the plate from one outer edge to another, but here the authors modeled half of the plate (i.e. modeled the plate from the center of the plates to the outer edge of the plates). This may reduced the number of nodes and thus reduce the cost of calculation time.

In the present paper, the problem is solved by using finite difference method (FDM). The governing equations and boundary conditions will be descretized by applications of the central difference approximations. The descretized equations along with the descretized boundary conditions will then formed a system of algebraic equations to be solved.

At the interface of circular and annular plate, the matching condition is imposed. As mentioned earlier, in application of central difference, there exists

phantom nodes outside the physical region. For finite different problem involving two different regions such as this problem, the phantom nodes of one region fell into another region. The phantom nodes one region will equal to nodes on another region if the meshing is equal in both regions. In the present study, the mesh is set to equal. In the present problem, the space between two nodes is defined by

$$r_{step} = \frac{2\,(r_o - r_i)}{2m+1} \tag{38}$$

where m is the number of nodes between nodes at inner edge and outer edge.

3.1 Treatment at Center of Circular Plate

Solving differential equation, such as the plate governing equation for disk, which use a polar coordinate pose a problem at the origin or the center of the plate since it is singular at that point. Some researchers proposed extra condition for the origin which would give a non-singular solution at the origin (Mohseni and Colonius, 2000). Lai (Lai, 2002) has proposed a very simple way to treat this problem. Lai (Lai, 2002) recognize that the numerical boundary condition at the origin (or the pole) in the traditional finite difference is needed only in the discretization of the transformed equation in the polar coordinate system. There is no need to impose any conditions from the rectangular coordinate point of view. He proposed a special mesh point locations so that this numerical boundary condition can be avoided. The special mesh points is achieved by shifting a grid a half mesh away from the origin and incorporating the symmetry constraint of Fourier coefficients. This approach also does not need to use one sided difference approximation (i.e. backward difference approximation) at the origin. The similar approach also reported by Mohseni and Colonius (Mohseni and Colonius, 2000).

4. Results and Discussions

The properties of piezoceramic material and the isotropic alloy are summarized in Table 1 and Table 2, respectively. Aung and Wang (Aung and Wang, 2005) has reported a circular plate buckling problems due to intermediate radial edge. However in their report, the stress distribution at annular plate is assumed either uniform throughout the annular plate or stress free. This is not the case if the annular plate is constrained with two different conditions along its two edges. For the stress to be uniform throughout the annular plate, the in-plane load has to be equal at both of its edge and for the annular plate to be stress free, it has to be constrained so that the annular plate behave like a

Table 1: Material Properties of Piezoceramic PIC-151

Property	Value
s_{11}^E $(10^{-12}\ m^2/N)$	16.83
s_{33}^E	19.0
s_{12}^E	-5.656
s_{13}^E	-7.107
s_{44}^E	50.96
s_{66}^E	44.97
d_{31} $(10^{-10}$ m/V)	-2.14
d_{33}	4.23
d_{15}	6.1
ϵ_{11}^T $(10^{-9}$ F/m)	17.134
ϵ_{33}^T	18.665

Table 2: Material Properties of Brass Alloy

Property	Value
E $(10^9\ N/m^2)$	110
μ	0.34

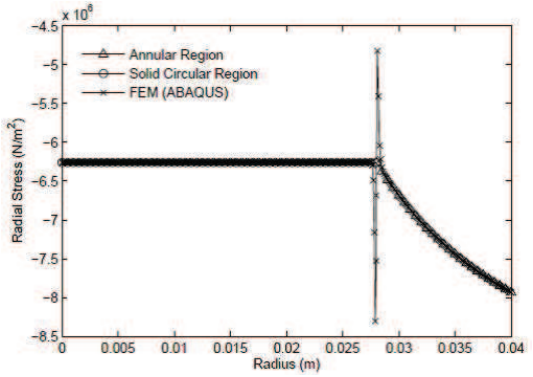

Figure 2: Radial stress distribution with applied voltage is 200 V

rigid body. Fig. 2 shows the comparison of the determined stress variation with the one obtained from FEM analysis. The results shows excellent agreement between the two results except at very narrow region at the annular-circular interface. The authors believe this is due to the boundary layer effects at an interface of two different regions with different properties.

In the present case, which the author believe to be the case for many practical cases due to intermediate radial load, the stress is varied with radius. This is due to the fact that the radial load is different for both inner and outer edge.

The FEM analysis is done by using FEM software (ABAQUS) where the plate is modeled by using axisymmetric element (8-node biquadratic axisymmetric quadrilateral, reduced integration (CAX8R) for isotropic alloy region and 8-node biquadratic axisymmetric piezoelectric quadrilateral, reduced integration (CAX8RE) is used for piezoceramic region). The FDM is formulated as discussed in Section 3 and coded in MATLAB. The number of nodes at the annular regions, m is 150 nodes. The number of nodes at the circular region varies as the inner edge varies. Table 3-5 shows the critical buckling loads compared to the one found by FEM analysis.

Table 3: Critical buckling voltage for circular and annular plates having equal thicknesses

Mode (nodal circle)	FDM (Hz)	FEM (Hz)	Error (%)
1 (1)	245.93	235.00	4.44
2 (2)	844.10	825.27	2.23
3 (3)	1747.10	1713.60	1.92
4 (4)	2987.10	2945.30	1.40

Table 4: Critical buckling voltage for annular plates is thicker than circular plate

Mode (nodal circle)	FDM (Hz)	FEM (Hz)	Error (%)
1 (1)	742.20	725.85	2.20
2 (2)	2366.20	2296.30	2.95
3 (3)	4397.70	4239.20	3.60
4 (4)	6860.60	6703.40	2.29

Table 5: Critical buckling voltage for circular plates is thicker than annular plate

Mode (nodal circle)	FDM (Hz)	FEM (Hz)	Error (%)
1 (1)	671.00	650.90	3.00
2 (2)	1654.50	1602.60	3.14
3 (3)	4398.80	4324.30	1.69
4 (4)	6862.10	6804.20	0.84

Fig. 3, Fig. 4, and Fig. 5 shows some of the parametric study. Fig. 3 shows how the critical buckling voltage change with the inner radius. Other parameters is fixed. Outer radius, r_1 is fixed at 40 mm while the annular and circular thicknesses are divided into 3 cases, (a.) same thickness at 0.3 mm, (b.)

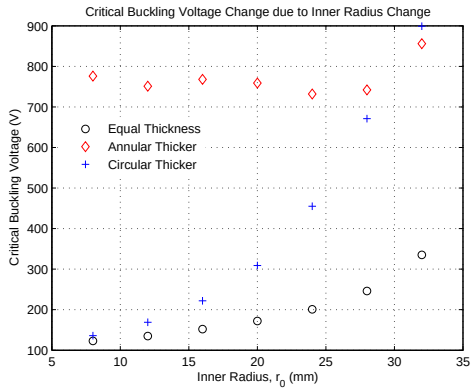

Figure 3: Critical Buckling Voltage change due to Inner Radius

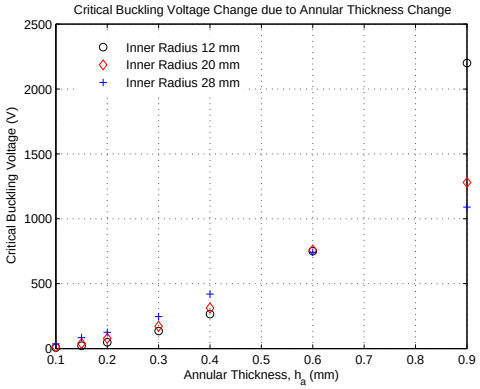

Figure 4: Critical Buckling Voltage change due to Annular Thickness

annular (0.6 mm) thicker than circular thickness (0.3 mm) and (c.) circular (0.6 mm) thicker than annular thickness (0.3 mm). The results for this configurations shows that for cases which annular that having similar thickness with circular and circular plate is thicker, the critical buckling voltage is increases with the inner radius. While for case which annular thicker than the circular plate, it seems that the inner radius change does not have significant effects in changing the buckling voltage. Also, one may notes that the inner radius have significant influence on the critical buckling voltage for the case of circular plate is thicker than the annular plate where the increase is rapid as the inner radius increase. Fig. 4 shows how the critical buckling voltage change with

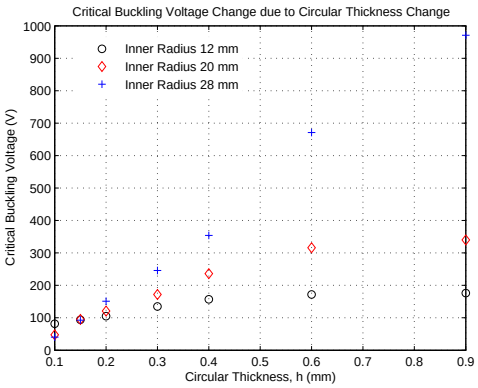

Figure 5: Critical Buckling Voltage change due to Circular Thickness

the annular thickness. The outer radius and circular thickness for this case are 40 mm and 0.3 mm, respectively. The inner radius are divided for 3 cases which are (a.) 12 mm, (b.) 20 mm and (c.) 28 mm. For this configuration the results shows that, for any inner radius, the critical buckling voltage increases as the annular thickness increases. Note that annular thickness more than 0.3 mm refers to annular plate is thicker than the circular thickness. Fig. 5 shows how the critical buckling voltage change with the annular thickness. The outer radius and annular thickness for this case are 40 mm and 0.3 mm, respectively. The inner radius are divided for 3 cases which are (a.) 12 mm, (b.) 20 mm and (c.) 28 mm. For this configuration one may see that, beyond the thickness around 0.4 mm, the critical buckling voltage almost unchanged as the circular thickness increases except when the inner radius is near to outer radius. Note that circular thickness more than 0.3 mm refers to circular plate is thicker than the annular thickness.

5. Conclusions

A buckling analysis of an isotropic circular plate with piezoceramic annular plate attached to it is presented. The annular plate is attached at the circular plate edge where the radius of the circular plate is the inner radius of the annular plate. The piezoceramic annular plate is used as the radial in-plane load source. The radial and hoop stresses are found to be depends on the radial throughout the annular region while contants throughout the circular regions. The governing equations is solved approximately using finite difference method. The solutions to be found to be in good agreement with results from FEM

analysis. A parametric study also has been conducted. It is found that the inner radius has a significant influence in critical buckling voltage except for the case of annular plate is thicker than the circular plate. Also, it is found that for inner radius far enough from the outer radius, the circular thickness only influence the critical buckling voltage when the circular plate has thickness near the annular plate or smaller. Lastly, the critical buckling voltage increases as the annular thickness increases regardless the annular plate is thicker or thinner than the circular plate.

References

Wang, C. M., Wang, C. Y., & Reddy, J. N. Exact solutions for buckling of structural members, 2005.

Mansfield, E. H. On the buckling of an annular plate. *Quarterly Journal of Mechanical Applied Mathematics*, 13(1):16–23, 1960.

Ramaiah, G. K. & Vijayakumar, K. Elastic stability of annular plates under uniform compressive forces along the outer edge. *AIAA Journal*, 13(6):832, 1974.

Sheng-li, Q. & Ai-shu, Z. On the problems of buckling of an annular thin plate. *Applied Mathematics and Mechanics (English Edition)*, 6(2):169–183, 1984.

Shi-rong, L. Nonlinear vibration and thermal-buckling of a heated annular plate with a rigid mass. *Applied Mathematics and Mechanics (English Edition)*, 13(8):771–777, 1992.

Kiang, F.-r. Some applications of perturbation method in thin plate bending problems. *Applied Mathematics and Mechanics (English Edition)*, 1(1):35–53, 1980.

Coman, C. D. & Haughton, D. M. On some approximate methods for the tensile instabilities of thin annular plates. *Journal of Engineering Mathematics*, 56: 79–99, 2006a.

Coman, C. D. & Haughton, D. M. Localized wrinkling instabilities in radially stretched annular thin films. *Acta Mechanica*, 185:179–200, 2006b.

Aung, T. M. & Wang, C. Buckling of circular plates under intermediate and edge radial loads. *Thin-Walled Structures*, 43:1926–1933, 2005.

Tiersten, H. F. *Linear Piezoelectric Plate Vibrations*. Plenum Press, 1969.

Wang, Q., Quek, S. T., Sun, C. T., & Liu, X. Analysis of piezoelectric coupled circular plate. *Smart Material and Structures*, 10:229–239, 2001.

Huang, C. H., Lin, Y. C., & Ma, C. C. Theoretical analysis and experimental measurement for resonant vibration of piezoceramic circular plates. *IEEE Transaction on Ultrasonics, Ferroelectrics, and Frequency Control*, 51(1):12–24, 2004.

Huang, C. H. Free vibration analysis of the piezoceramic bimorph with theoretical and experimental investigation. *IEEE Transactions on Ultrasonics, Ferroelectrics, and Frequency Control*, 52(8):1393–1403, 2005.

Mohseni, K. & Colonius, T. Numerical treatment of polar coordinate singularities. *Journal of Computational Physics*, 157:787–795, 2000.

Lai, M.-C. A simple compact fourth-order poisson solver on polar geometry. *Journal of Computational Physics*, 182:337–345, 2002.